THE JOURNAL OF PHYSICAL CHEMISTRY Letters

pubs.acs.org/JPCL Letter

Manipulating Two-Photon-Absorption of Cavity Polaritons by Entangled Light

Bing Gu* and Shaul Mukamel*

Cite This: J. Phys. Chem. Lett. 2020, 11, 8177–8182 Read Online

ACCESS | Metrics & More | Article Recommendations | Supporting Information

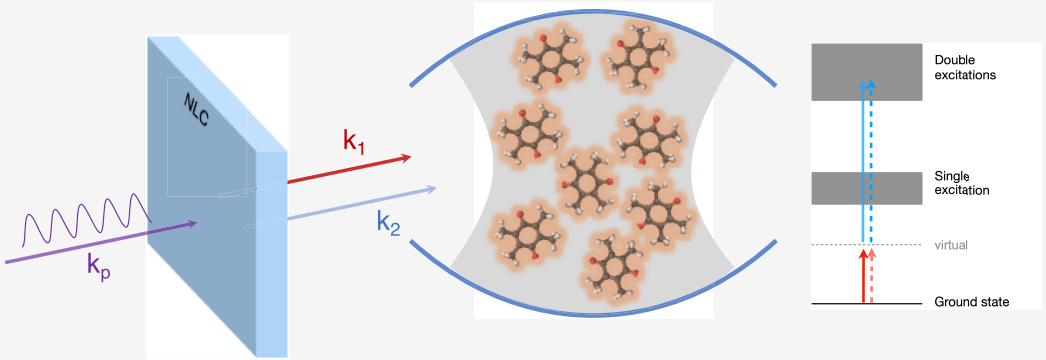

ABSTRACT: We demonstrate that two-photon excitations to bipolariton states created by placing several molecules in an optical cavity can be manipulated by quantum light. Entangled photons can access classically dark bipolariton states by modifying the quantum interferences of two-photon transition pathways involving different single-polariton intermediate states and time-ordering of the two photon beams.

Cavity polaritons are hybrid light−matter states that emerge in the strong coupling regime between material polarization and cavity photon modes. Polaritons have been experimentally demonstrated as a new means to modify the electronic, optical, and chemical properties of molecules by coupling to the vacuum field without external laser driving.[1−10] Nonlinear spectroscopic techniques such as pump−probe, transient absorption, two-dimensional infrared spectroscopy, and Raman scattering have been used for probing polaritons and their dynamics in complex molecular systems.[2,9,11−15] In other developments, employing quantum light in nonlinear molecular spectroscopy has opened up many novel opportunities to enhance the signal-to-noise ratio, the resolution, and the selectivity of transition pathways.[16−25] Photon entanglement offers a new and unique control knob that does not exist for classical laser pulses.

Here we show how to employ nonlinear quantum light spectroscopy for probing two-photon excitations in polaritonic systems. We theoretically investigate the combined signatures of a cavity photon mode strongly coupled to molecules and entangled photons[26] on collective bipolariton resonances. We study the two-photon absorption (TPA) signal with an entangled photon pair to a polaritonic system consisting of N two-level molecules strongly coupled to a single cavity photon mode. By comparing the TPA spectra with classical and quantum light, we demonstrate that entangled photons can create two-photon excitations in polaritonic systems that are drastically different from the classical two-photon excitations. Entangled photons can reveal classically dark bipolariton states by modifying the quantum interference among transtion pathways leading to TPA. The manipulation of double excitations in strongly coupled cavity−matter systems by quantum light can have many potential applications to polaritonic chemistry, sensing, and microscopy.

Atomic units ($\hbar = 1$) are used throughout.

Our system, sketched in Figure 1a, is described by the Hamiltonian $H = H_p + H_R + H_{RM}$. The polariton Hamiltonian

$$H_p = \sum_{n=1}^{N} \omega_n \sigma_n^\dagger \sigma_n + \omega_c a^\dagger a + \sum_{n=1}^{N} g_n(\sigma_n^\dagger + \sigma_n)(a + a^\dagger) \quad (1)$$

describes N two-level molecules strongly coupled to a single cavity mode with creation (annihilation) boson operators $a^\dagger$ (a) whereas $\sigma_n^\dagger$ and σ_n are the raising and lowering Pauli operators of the nth molecule, respectively. The probe radiation modes, described by $H_R = \sum_{k,\mu} \hbar\omega_k b_{k\mu}^\dagger b_{k\mu}$, drive the sample via the

Received: July 24, 2020
Accepted: September 2, 2020
Published: September 2, 2020

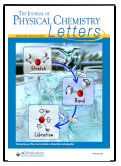

https://dx.doi.org/10.1021/acs.jpclett.0c02282
J. Phys. Chem. Lett. 2020, 11, 8177−8182

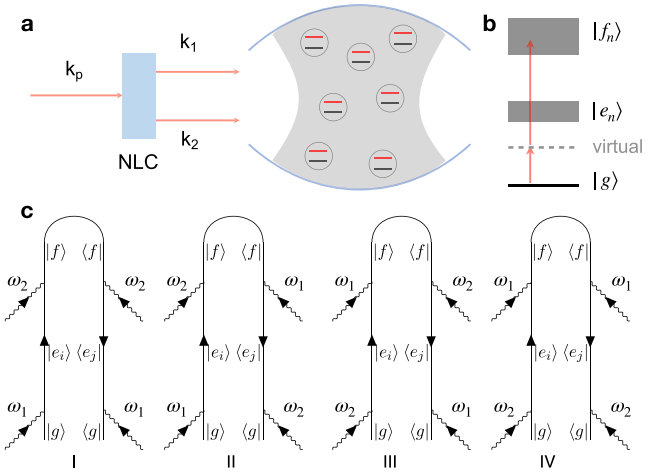

Figure 1. (a) Setup for probing polaritons with entangled TPA. A pump photon impinging a second-order nonlinear crystal (NLC) is down-converted into an entangled photon pair, which is then directed to the molecules embedded in an optical cavity. (b) The polariton energy level scheme. (c) Time-loop diagrams for the signal. There are four pathways depending on the sequence of photons that interact with the polariton system, represented by curly arrows along the time-loop. $|e_i\rangle$ and $|e_j\rangle$ run over the single-polariton states.

electric dipole operator in the rotating-wave approximation (in the interaction picture of $H_p + H_R$)

$$H_{RM}(t) = \sum_{j=1,2} V_j^\dagger(t)\hat{E}_j(t) + V_j(t)\hat{E}_j^\dagger(t) \tag{2}$$

where $\hat{E}_j(t) = i\int_0^\infty d\omega \sqrt{\frac{\hbar\omega}{2\mathcal{V}\epsilon_0}} b_j(\omega)e^{-i\omega t}$ is the positive-frequency component of the electric field operator of the jth photon beam with polarization $\mathbf{e}_j$ and $\mathcal{V}$ is the quantization volume; $V_j \propto \sum_n \sigma_n$ and $V_j^\dagger$ denote the lowering and raising dipole operator, respectively, for all molecules in the direction of the field polarization, i.e., $V_j + V_j^\dagger = -\boldsymbol{\mu}\cdot\mathbf{e}_j$. In eqs 1 and 2, we have assumed the sample size is much smaller than the wavelength of the cavity mode and the probe photon modes ($\lambda = 413$ nm for $\omega = 3$ eV), but the molecular separation is large enough such that a direct intermolecular coupling can be neglected.

When the polaritonic system is initially in the ground state $|g\rangle$ with no excitation in the molecules and cavity, the TPA signal is given by the transition probability of arriving at the final bipolariton states $|f\rangle$ in the double-excitation manifold (see Figure 1b for the level scheme)

$$P(t) = \sum_f \mathrm{Tr}\{|f\rangle\langle f|\rho(t)\} \tag{3}$$

where $\rho(t)$ is the joint density matrix of the molecules, cavity, and extra radiation modes. As shown in Section S1, the entangled TPA signal contains four contributions represented by the time-loop diagrams in Figure 1c

$$S_{ETPA} = \sum_{\mathbf{p}} \int_{t_0}^{t} dt_2 \int_{t_0}^{t_2} dt_1 \int_{t_0}^{t} dt_2' \int_{t_0}^{t_2'} dt_1' \, C_{\mathbf{p}}(t_1', t_2', t_2, t_1) \times G_{\mathbf{p}}^{(2)}(t_1', t_2', t_2, t_1) \tag{4}$$

where $C_{\mathbf{p}}(t_1', t_2', t_2, t_1) = \langle V_{p_4}(t_1')V_{p_3}(t_2')V_{p_2}^\dagger(t_2)V_{p_1}^\dagger(t_1)\rangle$ and $G_{\mathbf{p}}^{(2)}(t_1', t_2', t_2, t_1) = \langle \hat{E}_{p_4}^\dagger(t_1')\hat{E}_{p_3}^\dagger(t_2')\hat{E}_{p_2}(t_2)\hat{E}_{p_1}(t_1)\rangle$ are matter and field correlation functions, respectively; the subscript $\mathbf{p} = \{p_4p_3p_2p_1\}$ signifies the photon beams (ω_1 or ω_2) that interact with matter along the time-loop clockwise (p_1 interacts first, and p_4 the last). Equation 4 expresses the entangled TPA (ETPA) signal through a time-convolution of the four-point polariton and field correlation functions and holds for any factorized initial state of the polaritonic system and probe field. $C_{\mathbf{p}}$ contains the third-order response of the probed polaritonic system, whereas $G_{\mathbf{p}}^{(2)}$ represents the nonclassical nature of the entangled photon state and enables manipulation of optical signals through shaping the photon entanglement.[27]

If the initial state of the probe radiation modes is pure $|\Phi\rangle$, the ETPA signal can be recast as the modulus square of a transition amplitude $S_{ETPA} = \sum_f |T_{fg}|^2$ (Section S2) with

$$T_{fg}(t) = \sum_{p_1\neq p_2} \sum_e D_{p_2p_1}^{(e)} \int_{-\infty}^{t} dt_1 e^{-i\omega_{fg}t_1} \int_0^\infty d\tau \, e^{i\omega_e\tau}\langle 0|\hat{E}_{p_2}(t_1)\hat{E}_{p_1}(t_1-\tau)|\Phi\rangle \tag{5}$$

where $D_{ij}^{(e)} \equiv (\boldsymbol{\mu}_{fe}\cdot\mathbf{e}_i)(\boldsymbol{\mu}_{eg}\cdot\mathbf{e}_j)$, $|0\rangle$ is the vacuum. The field transition amplitude further factorizes for classical light $\langle 0|\hat{E}_{p_2}(t_2)\hat{E}_{p_1}(t_1)|\Phi\rangle = E_{p_2}(t_2)E_{p_1}(t_1)$; see Table S1 for a comparison of time-domain and frequency-domain expressions for classical and quantum light.

We consider entangled photons created by a parametric down-conversion process whereby a pump photon splits into a pair of entangled twin-photons by interaction with a second-order nonlinear crystal. The two-mode squeezed state of the twin-photon, labeled 1 and 2, reads

$$|\Phi\rangle = \iint d\omega_1 d\omega_2 \phi(\omega_1, \omega_2) b_1^\dagger(\omega_1) b_2^\dagger(\omega_2)|0\rangle \tag{6}$$

where the joint spectral amplitude $\phi(\omega_1, \omega_2)$ depends on the entanglement time T, pump photon frequency ω_p, and the central frequencies of the output photon beams ω_j^0. For a monochromatic pump[28]

$$\phi(\omega_1, \omega_2) = \mathcal{N}\delta(\omega_1 + \omega_2 - \omega_p)\mathrm{sinc}(\Delta\omega_1 T/2) \tag{7}$$

where T is the entanglement time characterizing the transit time difference of twin photons, $\Delta\omega_1 = \omega_1 - \omega_1^0 = -\Delta\omega_2$, and $\mathcal{N}$ is a normalization factor (see Section S3). Transforming the joint spectral amplitude to the time domain and inserting it in eq 5 yields

$$T_{fg} = \frac{\pi\mathcal{N}\sqrt{\omega_1^0\omega_2^0}}{\epsilon_0\mathcal{V}T(\omega_{fg} - i\gamma_f - \omega_1^0 - \omega_2^0)} \sum_e \sum_{p_1\neq p_2} D_{p_2p_1}^{(e)} \times \frac{1 - \exp[-i(\Delta_e^{(p_1)} - i\gamma_e)T/2]}{\Delta_e^{(p_1)} - i\gamma_e} \tag{8}$$

where $\Delta_e^{(n)} = \omega_{eg} - \omega_n^0$ is the detuning between the transition energy to the intermediate state and the central frequency of the photon beam. The prefactor in eq 8 $(\omega_1^0 + \omega_2^0 - \omega_{fg} + i\gamma_f)^{-1}$ contains the two-photon resonances. The ETPA transition pathways are modulated by a factor of $1 - e^{-i\Delta_e^{(n)}T/2}$, which depends on the entanglement time T and the detuning $\Delta_e^{(p_1)}$. For long entanglement times, $\lim_{T\to\infty} e^{-i(\Delta_e^{(n)} - i\gamma_e)T/2} = 0$ and eq 8 reduces to the classical form

https://dx.doi.org/10.1021/acs.jpclett.0c02282
J. Phys. Chem. Lett. 2020, 11, 8177−8182

$$T_{fg}^{\mathrm{cl}} = \frac{E_1(\omega_1^0)E_2(\omega_2^0)}{\omega_{fg} - i\gamma_f - \omega_1^0 - \omega_2^0} \sum_e \sum_{p_1 \neq p_2} \frac{D_{p_2 p_1}^{(e)}}{\Delta_e^{(p_1)} - i\gamma_e} \tag{9}$$

In this limit, the time-correlation of the photon pair is lost: the arrival of one photon carries no information about the arrival time of its twin.

It is instructive to consider first a polaritonic system with two molecules, a and b with $\omega_c = (\omega_a + \omega_b)/2$, which has three *e*-states and four *f*-states (Figure 2a). The polariton eigenstates are

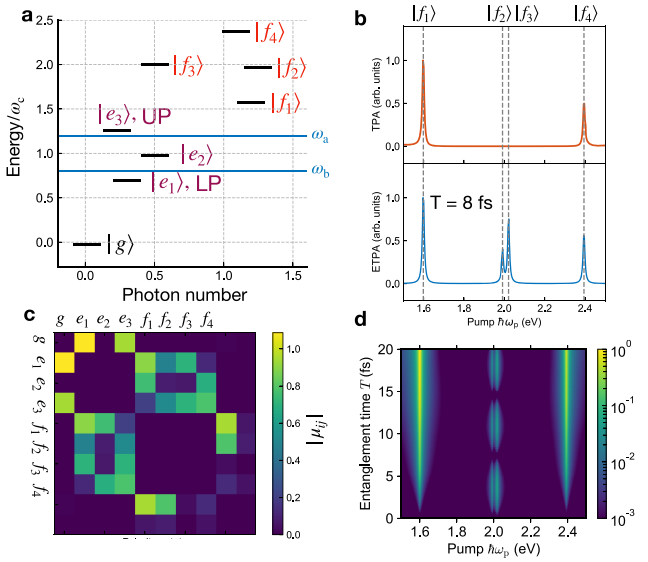

Figure 2. Two-photon absorption signal (TPA) for two two-level molecules interacting with a single cavity mode. (a) Polariton energy levels. The cavity photon number $\langle\Psi|a^\dagger a|\Psi\rangle$ is given for each polariton state $|\Psi\rangle$. (b) TPA with (upper panel) classical light and (lower panel) entangled photon pair with entanglement time $T = 8$ fs. The spectra are normalized to have the same maximum intensity 1. (c) Transition dipole moment. (d) Entangled TPA versus the entanglement time T. The middle bipolariton peaks oscillate with T, and its relative intensity over the upper/lower bipolariton state is higher at short entanglement times. Here $\omega_a/\omega_c = 0.8$, $\omega_b/\omega_c = 1.2$, $\omega_1^0 = \omega_2^0 = \omega_p/2$, and $g_a = g_b = 0.14$ eV.

obtained by diagonalizing the Hamiltonian matrix represented in terms of the direct product basis $|ijn\rangle \equiv |i\rangle_a \otimes |j\rangle_b \otimes |n\rangle_c$. The single-excitation manifold contains the upper and lower polariton states $|e_1\rangle$, $|e_3\rangle$ and one dark polariton state $|e_2\rangle$. The Hamiltonian in the single-excitation block spanned by $\{|gg1\rangle, |eg0\rangle, |ge0\rangle\}$ (eq S48) leads to the single-polariton eigenstates

$$\begin{bmatrix} |e_3\rangle \\ |e_2\rangle \\ |e_1\rangle \end{bmatrix} = \begin{bmatrix} \frac{1}{\sqrt{2}}\sin\theta & \cos^2\left(\frac{\theta}{2}\right) & \sin^2\left(\frac{\theta}{2}\right) \\ \cos\theta & -\frac{1}{\sqrt{2}}\sin\theta & \frac{1}{\sqrt{2}}\sin\theta \\ -\frac{1}{\sqrt{2}}\sin\theta & \sin^2\left(\frac{\theta}{2}\right) & \cos^2\left(\frac{\theta}{2}\right) \end{bmatrix} \begin{bmatrix} |gg1\rangle \\ |eg0\rangle \\ |ge0\rangle \end{bmatrix} \tag{10}$$

where $\delta = \omega_a - \omega_c$ and $\theta = \arctan\frac{\sqrt{2}g}{\delta} \in [0, \pi]$. The state $|e_2\rangle$ lies at the cavity resonance $\omega_{e_2} = \omega_c$, whereas $|e_1\rangle$ and $|e_3\rangle$, $\omega_{e_3/e_1} = \omega_c \pm \sqrt{\delta^2 + 2g^2}$, are separated by $2\sqrt{\delta^2 + 2g^2} \geq 2\sqrt{2}g$. At $\delta = 0$, $|e_2\rangle$ reduces to the dark exciton state $|X_-\rangle = \frac{1}{\sqrt{2}}(|ge0\rangle - |eg0\rangle)$, and the Rabi splitting reduces to the cooperative Rabi splitting for a homogeneous system $2g\sqrt{N}$ with $N = 2$. The splitting increases with the detuning δ.

The double-excitation block Hamiltonian within the rotating-wave approximation neglecting counter-rotating terms $\sum_{n=1}^{N} g_n(a^\dagger\sigma_n^\dagger + \mathrm{H.c.})$ in cavity−molecule coupling is spanned by the basis set $|gg2\rangle$, $|eg1\rangle$, $|ge1\rangle$, $|ee0\rangle$ (eq S42) and contains two degenerate middle bipolariton states $|f_2\rangle$, $|f_3\rangle$) at $2\omega_c$

$$\begin{aligned} |f_2\rangle &= [0, 1/\sqrt{2}, -1/\sqrt{2}, -\eta]/\sqrt{1+\eta^2} \\ |f_3\rangle &= [\eta, -1, 1, 0]/\sqrt{\eta^2 + 2} \end{aligned} \tag{11}$$

where $\eta = \delta/(\sqrt{2}g)$. The $|f_1\rangle/|f_4\rangle$ splitting $2\sqrt{\delta^2 + 6g^2}$ is larger than the vacuum Rabi splitting $2\sqrt{\delta^2 + 2g^2}$. For vanishing cavity−molecule coupling $g = 0$, $|f_2\rangle$ and $|f_3\rangle$ reduce to the bare two-atom resonance state $|ee0\rangle$ and the two-cavity photon state $|2\rangle_c$, respectively. At zero detuning, they both collapse to $|X_-\rangle$ even for $g \neq 0$. The counter-rotating terms couple $|ge1\rangle$, $|eg1\rangle$ to the ground state $|gg0\rangle$, which breaks the degeneracy of $|f_2\rangle$ and $|f_3\rangle$ as shown in Figure 2a.

The classical TPA signal shown in Figure 2b (top) contains two peaks separated by a splitting much larger than the vacuum Rabi splitting, which correspond to the lowest and highest bipolariton states $|f_1\rangle$ and $|f_4\rangle$. The states $|f_2\rangle$ and $|f_3\rangle$ are two-photon allowed because the system can undergo a one-photon transition to $|e_1\rangle$ or $|e_3\rangle$ ($|e_2\rangle$ is dark) and then absorb a second photon to the final state (see Figure 2c for the matrix elements of the transition dipole). One would thus expect to observe such bipolariton resonances in the TPA spectrum. However, these resonances cancel out by destructive interference of the four transition pathways (Figure 1c).

The transition amplitude for $|g\rangle \xrightarrow{\text{photon 1}} |e_3\rangle \xrightarrow{\text{photon 2}} |f\rangle$ (pathway I) has opposite sign to $|g\rangle \xrightarrow{\text{photon 2}} |e_1\rangle \xrightarrow{\text{photon 1}} |f\rangle$ (II). These read

$$T^{(\mathrm{I})} = \frac{\mu_{f,e_3}\mu_{e_3,g}}{\Delta_{e_3}^{(1)} - i\gamma_{e_3}}, \qquad T^{(\mathrm{II})} = \frac{\mu_{f,e_1}\mu_{e_1,g}}{\Delta_{e_1}^{(2)} - i\gamma_{e_1}} \tag{12}$$

The interference is destructive for bipolariton states with eigenenergies $\omega_f \approx \omega_{e_1} + \omega_{e_3}$. First, $\omega_1 + \omega_2 = \omega_f \approx \omega_{e_3} + \omega_{e_1}$ leads to $\Delta_{e_3}^{(1)} \approx -\Delta_{e_1}^{(2)}$. Additionally, if the matrix elements of the transition dipole satisfy $\mu_{f_2,e_3}\mu_{e_3,g} = \mu_{f_2,e_1}\mu_{e_1,g}$, it follows that

$$T^{(\mathrm{I})} + T^{(\mathrm{II})} \approx 0 \tag{13}$$

Similarly, the other two transition pathways also cancel out. The total transition amplitude to $|f\rangle$ vanishes. Consequently, $|f_2\rangle$ and $|f_3\rangle$ are dark in the classical TPA spectrum. For noninteracting molecules without the cavity, this interference leads to the vanishing of collective two-photon resonance,[29,29−32] reflecting the fact that classical light cannot create correlations between molecules. The picture is very different for polaritons where the molecules are effectively coupled through the cavity mode leading to bipolariton resonances in the TPA even with classical light.

We now discuss how an entangled photon pair modifies the quantum interference and reveals dark bipolariton states. The

https://dx.doi.org/10.1021/acs.jpclett.0c02282
J. Phys. Chem. Lett. 2020, 11, 8177−8182

ETPA spectrum for the entanglement time $T = 8$ fs (Figure 2b, bottom) differs from the classical signal by two extra bipolariton resonances around $\omega = \omega_{e_1} + \omega_{e_3} = 2$ eV. As discussed above, such states are dark because of destructive interference. However, entangled photons allow different two-photon excitation selection rules than classical light. For short entanglement times, $\Delta_e^{(n)} T \ll 1$ where the arrival of photon 1 implies the arrival of photon 2 within a short period of time. The transition amplitude eq 8 becomes

$$T_{fg} = \frac{i\pi \mathcal{N}\sqrt{\omega_1^0 \omega_2^0}}{2\epsilon_0 \mathcal{V}(\omega_{fg} - i\gamma_f - \omega_1^0 - \omega_2^0)} \sum_e \sum_{p_1 \neq p_2} D^{(e)}_{p_2 p_1} \tag{14}$$

In this limit, the transition amplitude does not depend on the detuning between the incoming photon and the intermediate state and destructive interference can become constructive. This is reflected in the variation of the ETPA spectrum with the entanglement time T shown in Figure 2d. The $|f_2\rangle$ and $|f_3\rangle$ peaks oscillate with T showing that interference is changing between destructive and constructive with the entanglement time T. The relative intensity of $|f_2\rangle$ compared to $|f_1\rangle$ and $|f_4\rangle$ is most pronounced for short entanglement times T and decreases with T.

For a system with N identical molecules, the bipolariton block Hamiltonian can be decomposed into three subblocks (see Section S4.B for a detailed analysis of the bipolariton manifold). As shown in Figure 3b for $N = 8$, there is one collective

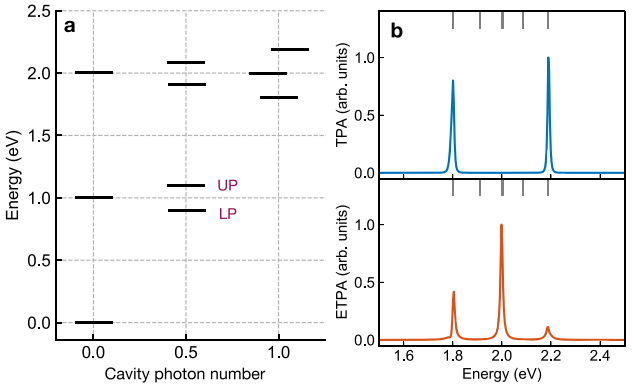

Figure 3. TPA of $N = 8$ identical molecules in an optical cavity, calculated with counter-rotating terms in the cavity−molecule coupling. (a) Single- and bipolariton eigenstates. (b) Comparison between the TPA with (upper panel) classical light and with (lower panel) entangled photons $T = 8$ fs. Here $\omega_0 = \omega_c = 1$ eV, $g_0\sqrt{N} = 0.2$ eV. The upper and lower single-polaritons (UP/LP) act as intermediate states.

bipolariton, an entangled state involving all molecules plus cavity photon, that cannot be revealed by classical TPA due to destructive interference between transition pathways where the collective UP and LP act as intermediate states. This resonance can be observed by employing entangled photons. There are $\frac{1}{2}N(N+1)$ bipolaritons and $N+1$ single-polariton states for N two-level molecules coupled to a cavity mode. The reasons why the TPA signal contains only a few resonances are due to (i) the large degeneracy of bipolaritons and (ii) the fact that there are only two bright single-polaritons, UP and LP, in this ideal limit of identical molecules, meaning that only bipolaritons that are coupled to UP/LP will be observed. Similar spectra are observed for $N > 8$.

We now consider a system with eight molecules with disordered transition frequencies due to, for example, local environments $\omega_j = \omega_0 + \sigma\eta_j$. Here, $\eta_j = \mathcal{N}(0,1)$ is a random variable with normal distribution and σ is the disorder strength. The two columns in Figure 4 present the TPA spectrum for two

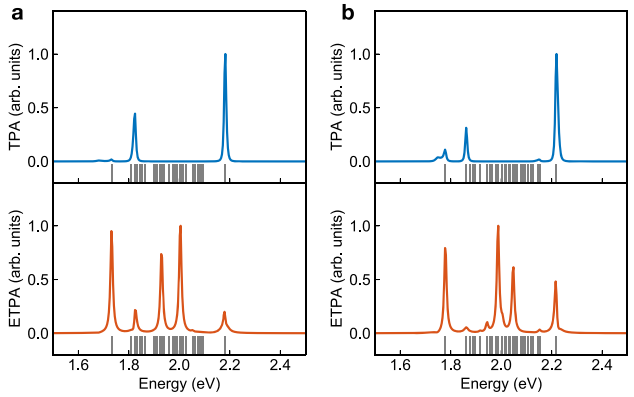

Figure 4. Comparison of the classical TPA and ETPA of $N = 8$ molecules with disordered transition frequencies in an optical cavity. The ETPA signal is generated by the twin photons with entanglement time $T = 8$ fs. The molecular transition energies are $\omega_j = \omega_0 + \sigma\eta_j$, $\sigma = 0.02$ eV. The two columns represent two realizations of $\eta_j = \mathcal{N}(0,1)$, normally distributed random energies.

realizations of η_j. TPA spectra for $N > 8$ molecules exhibit similar features, despite a larger bipolariton manifold. Entangled photons induce additional bipolariton resonances than classical light. A disordered system has many more bright single polaritons than just the UP and LP as for identical molecules, and the degeneracies of bipolariton states are lifted. The number of transition pathways that needs to be taken into account for one bipolariton is twice the number of bright single-polaritons because of the time-ordering of the interacting photons. Even for a single molecule, there are four transition pathways that offer the opportunity for manipulating the two-photon excitations by entangled photons.

In summary, we have demonstrated how the TPA signal with quantum light can be used for probing cavity polaritons. The TPA spectra with an entangled photon pair and with classical light are compared for a strongly coupled cavity−molecule system. We found that while some collective bipolariton resonances are visible with classical light, many states in the double-excitation manifold are dark because of destructive interference among transition pathways. This interference can be manipulated by entangled light. Classically dark states can become bright by employing a parametric down-conversion generated entangled photon pair, which can turn the destructive into constructive interference.

While polariton chemistry studies have focused on the single-polariton subspace,[11,33−38] bipolaritons contain additional features such as enhanced splitting[39] and cooperative effects. There are many opportunities for employing nonlinear quantum light signals[20] for probing bipolariton and even higher-lying polariton states and tracking polariton dynamics. Photon entanglement offers unique control knobs for probing classical forbidden states by breaking some selection rules associated with classical light.[20] Future prospects involve investigating the

https://dx.doi.org/10.1021/acs.jpclett.0c02282
J. Phys. Chem. Lett. 2020, 11, 8177−8182

influence of electronic decoherence,[40,41] cavity loss, pulse shaping,[42] and chemical reactions.

■ ASSOCIATED CONTENT

Supporting Information

The Supporting Information is available free of charge at https://pubs.acs.org/doi/10.1021/acs.jpclett.0c02282.

Derivations of eqs 4, 5, and 7; time-domain and frequency-domain expressions for the two-photon absorption signal; bipolariton manifold of N two-level molecules interacting with a single cavity mode (PDF)

■ AUTHOR INFORMATION

Corresponding Authors

Bing Gu − *Department of Chemistry and Department of Physics and Astronomy, University of California, Irvine, California 92697, United States;* orcid.org/0000-0002-5787-3334; Email: bingg@uci.edu

Shaul Mukamel − *Department of Chemistry and Department of Physics and Astronomy, University of California, Irvine, California 92697, United States;* orcid.org/0000-0002-6015-3135; Email: smukamel@uci.edu

Complete contact information is available at: https://pubs.acs.org/10.1021/acs.jpclett.0c02282

Notes

The authors declare no competing financial interest.

■ ACKNOWLEDGMENTS

We thank Dr. Stefano M. Cavaletto, Dr. Wei Xiong, and Dr. Feng Chen for helpful discussions. We also thank Dr. Yiwen E for the schematic graphics. This work is supported by the National Science Foundation Grant CHE-1953045.

■ REFERENCES

(1) Ebbesen, T. W. Hybrid Light−Matter States in a Molecular and Material Science Perspective. *Acc. Chem. Res.* **2016**, *49*, 2403−2412.

(2) Shalabney, A.; George, J.; Hutchison, J.; Pupillo, G.; Genet, C.; Ebbesen, T. W. Coherent Coupling of Molecular Resonators with a Microcavity Mode. *Nat. Commun.* **2015**, *6*, 5981.

(3) Thomas, A.; Lethuillier-Karl, L.; Nagarajan, K.; Vergauwe, R. M. A.; George, J.; Chervy, T.; Shalabney, A.; Devaux, E.; Genet, C.; Moran, J.; Ebbesen, T. W. Tilting a Ground-State Reactivity Landscape by Vibrational Strong Coupling. *Science* **2019**, *363*, 615−619.

(4) Zhong, X.; Chervy, T.; Wang, S.; George, J.; Thomas, A.; Hutchison, J. A.; Devaux, E.; Genet, C.; Ebbesen, T. W. Non-Radiative Energy Transfer Mediated by Hybrid Light-Matter States. *Angew. Chem.* **2016**, *128*, 6310−6314.

(5) Zhong, X.; Chervy, T.; Zhang, L.; Thomas, A.; George, J.; Genet, C.; Hutchison, J. A.; Ebbesen, T. W. Energy Transfer between Spatially Separated Entangled Molecules. *Angew. Chem., Int. Ed.* **2017**, *56*, 9034−9038.

(6) Hutchison, J. A.; Schwartz, T.; Genet, C.; Devaux, E.; Ebbesen, T. W. Modifying Chemical Landscapes by Coupling to Vacuum Fields. *Angew. Chem., Int. Ed.* **2012**, *51*, 1592−1596.

(7) Orgiu, E.; George, J.; Hutchison, J. A.; Devaux, E.; Dayen, J. F.; Doudin, B.; Stellacci, F.; Genet, C.; Schachenmayer, J.; Genes, C.; Pupillo, G.; Samorì, P.; Ebbesen, T. W. Conductivity in Organic Semiconductors Hybridized with the Vacuum Field. *Nat. Mater.* **2015**, *14*, 1123−1129.

(8) Schwartz, T.; Hutchison, J. A.; Léonard, J.; Genet, C.; Haacke, S.; Ebbesen, T. W. Polariton Dynamics under Strong Light−Molecule Coupling. *ChemPhysChem* **2013**, *14*, 125−131.

(9) Xiang, B.; Ribeiro, R. F.; Du, M.; Chen, L.; Yang, Z.; Wang, J.; Yuen-Zhou, J.; Xiong, W. Intermolecular Vibrational Energy Transfer Enabled by Microcavity Strong Light− Matter Coupling. *Science* **2020**, *368*, 665−667.

(10) DelPo, C. A.; Kudisch, B.; Park, K. H.; Khan, S.-U.-Z.; Fassioli, F.; Fausti, D.; Rand, B. P.; Scholes, G. D. Polariton Transitions in Femtosecond Transient Absorption Studies of Ultrastrong Light−Molecule Coupling. *J. Phys. Chem. Lett.* **2020**, *11*, 2667−2674.

(11) Xiang, B.; Ribeiro, R. F.; Dunkelberger, A. D.; Wang, J.; Li, Y.; Simpkins, B. S.; Owrutsky, J. C.; Yuen-Zhou, J.; Xiong, W. Two-Dimensional Infrared Spectroscopy of Vibrational Polaritons. *Proc. Natl. Acad. Sci. U. S. A.* **2018**, *115*, 4845−4850.

(12) Dunkelberger, A. D.; Spann, B. T.; Fears, K. P.; Simpkins, B. S.; Owrutsky, J. C. Modified Relaxation Dynamics and Coherent Energy Exchange in Coupled Vibration-Cavity Polaritons. *Nat. Commun.* **2016**, *7*, 13504.

(13) Virgili, T.; Coles, D.; Adawi, A. M.; Clark, C.; Michetti, P.; Rajendran, S. K.; Brida, D.; Polli, D.; Cerullo, G.; Lidzey, D. G. Ultrafast Polariton Relaxation Dynamics in an Organic Semiconductor Microcavity. *Phys. Rev. B: Condens. Matter Mater. Phys.* **2011**, *83*, 245309.

(14) Ribeiro, R. F.; Campos-Gonzalez-Angulo, J. A.; Giebink, N. C.; Xiong, W.; Yuen-Zhou, J. Enhanced Optical Nonlinearities under Strong Light-Matter Coupling. *ArXiv (Phys. Physicsquant-Ph)* **2020**, 200608519.

(15) Wang, K.; Seidel, M.; Nagarajan, K.; Chervy, T.; Genet, C.; Ebbesen, T. W. Large Optical Nonlinearity Enhancement under Electronic Strong Coupling. *ArXiv (Phys.)* **2020**, 200513325.

(16) Mukamel, S. Roadmap on Quantum Light Spectroscopy. *J. Phys. B: At., Mol. Opt. Phys.* **2020**, *53*, 072002.

(17) Ficek, Z.; Drummond, P. D. Three-Level Atom in a Broadband Squeezed Vacuum Field. I. General Theory. *Phys. Rev. A: At., Mol., Opt. Phys.* **1991**, *43*, 6247−6257.

(18) Gea-Banacloche, J. Two-Photon Absorption of Nonclassical Light. *Phys. Rev. Lett.* **1989**, *62*, 1603−1606.

(19) Gardiner, C. W. Inhibition of Atomic Phase Decays by Squeezed Light: A Direct Effect of Squeezing. *Phys. Rev. Lett.* **1986**, *56*, 1917−1920.

(20) Dorfman, K. E.; Schlawin, F.; Mukamel, S. Nonlinear Optical Signals and Spectroscopy with Quantum Light. *Rev. Mod. Phys.* **2016**, *88*, 045008.

(21) Schlawin, F.; Dorfman, K. E.; Fingerhut, B. P.; Mukamel, S. Suppression of Population Transport and Control of Exciton Distributions by Entangled Photons. *Nat. Commun.* **2013**, *4*, 1782 DOI: 10.1038/ncomms2802.

(22) Lee, D.-I.; Goodson, T. Entangled Photon Absorption in an Organic Porphyrin Dendrimer. *J. Phys. Chem. B* **2006**, *110*, 25582−25585.

(23) Guzman, A. R.; Harpham, M. R.; Süzer, Ö.; Haley, M. M.; Goodson, T. G. Spatial Control of Entangled Two-Photon Absorption with Organic Chromophores. *J. Am. Chem. Soc.* **2010**, *132*, 7840−7841.

(24) Varnavski, O.; Pinsky, B.; Goodson, T. Entangled Photon Excited Fluorescence in Organic Materials: An Ultrafast Coincidence Detector. *J. Phys. Chem. Lett.* **2017**, *8*, 388−393.

(25) Georgiades, N. P.; Polzik, E. S.; Edamatsu, K.; Kimble, H. J.; Parkins, A. S. Nonclassical Excitation for Atoms in a Squeezed Vacuum. *Phys. Rev. Lett.* **1995**, *75*, 3426−3429.

(26) Rubin, M. H.; Klyshko, D. N.; Shih, Y. H.; Sergienko, A. V. Theory of Two-Photon Entanglement in Type-II Optical Parametric down-Conversion. *Phys. Rev. A: At., Mol., Opt. Phys.* **1994**, *50*, 5122−5133.

(27) Roslyak, O.; Mukamel, S. A Unified Description of Sum Frequency Generation, Parametric down Conversion and Two-Photon Fluorescence. *Mol. Phys.* **2009**, *107*, 265−280.

(28) Schlawin, F.; Dorfman, K. E.; Mukamel, S. Entangled Two-Photon Absorption Spectroscopy. *Acc. Chem. Res.* **2018**, *51*, 2207−2214.

(29) Muthukrishnan, A.; Agarwal, G. S.; Scully, M. O. Inducing Disallowed Two-Atom Transitions with Temporally Entangled Photons. *Phys. Rev. Lett.* **2004**, *93*, 093002.

(30) Mukamel, S. Communication: The Origin of Many-Particle Signals in Nonlinear Optical Spectroscopy of Non-Interacting Particles. *J. Chem. Phys.* **2016**, *145*, 041102.
(31) Zheng, Z.; Saldanha, P. L.; Rios Leite, J. R.; Fabre, C. Two-Photon− Two-Atom Excitation by Correlated Light States. *Phys. Rev. A: At., Mol., Opt. Phys.* **2013**, *88*, 033822.
(32) Richter, M.; Mukamel, S. Collective Two-Particle Resonances Induced by Photon Entanglement. *Phys. Rev. A: At., Mol., Opt. Phys.* **2011**, *83*, 063805.
(33) Gu, B.; Mukamel, S. Manipulating Nonadiabatic Conical Intersection Dynamics by Optical Cavities. *Chem. Sci.* **2020**, *11*, 1290−1298.
(34) Gu, B.; Mukamel, S. Cooperative Conical Intersection Dynamics of Two Pyrazine Molecules in an Optical Cavity. *J. Phys. Chem. Lett.* **2020**, *11*, 5555−5562.
(35) Kowalewski, M.; Mukamel, S. Manipulating Molecules with Quantum Light. *Proc. Natl. Acad. Sci. U. S. A.* **2017**, *114*, 3278−3280.
(36) Galego, J.; Garcia-Vidal, F. J.; Feist, J. Many-Molecule Reaction Triggered by a Single Photon in Polaritonic Chemistry. *Phys. Rev. Lett.* **2017**, *119*, 136001.
(37) Galego, J.; Climent, C.; Garcia-Vidal, F. J.; Feist, J. Cavity Casimir-Polder Forces and Their Effects in Ground-State Chemical Reactivity. *Phys. Rev. X* **2019**, *9*, 021057.
(38) Mandal, A.; Huo, P. Investigating New Reactivities Enabled by Polariton Photochemistry. *J. Phys. Chem. Lett.* **2019**, *10*, 5519−5529.
(39) Fink, J. M.; Göppl, M.; Baur, M.; Bianchetti, R.; Leek, P. J.; Blais, A.; Wallraff, A. Climbing the Jaynes−Cummings Ladder and Observing Its Nonlinearity in a Cavity QED System. *Nature* **2008**, *454*, 315−318.
(40) Gu, B.; Franco, I. Generalized Theory for the Timescale of Molecular Electronic Decoherence in the Condensed Phase. *J. Phys. Chem. Lett.* **2018**, *9*, 773−778.
(41) Gu, B.; Franco, I. Quantifying Early-Time Quantum Decoherence Dynamics through Fluctuations. *J. Phys. Chem. Lett.* **2017**, *8*, 4289−4294.
(42) Cao, J.; Che, J.; Wilson, K. R. Intrapulse Dynamical Effects in Multiphoton Processes: Theoretical Analysis. *J. Phys. Chem. A* **1998**, *102*, 4284−4290.

https://dx.doi.org/10.1021/acs.jpclett.0c02282
J. Phys. Chem. Lett. 2020, 11, 8177−8182

Supporting Information: Manipulating Two-Photon-Absorption of Cavity Polaritons by Entangled Light

Bing Gu* and Shaul Mukamel†

Department of Chemistry and Department of Physics and Astronomy, University of California, Irvine, CA 92697, USA

* bingg@uci.edu

† smukamel@uci.edu

CONTENTS

S1. EQ. 4 - ENTANGLED TWO-PHOTON-ABSORPTION

The two-photon absorption (TPA) signal is defined by the transition probability to a final state $|f\rangle$. In the interaction picture using $H_0 = H_\mathrm{p} + H_\mathrm{R}$,

$$P_f(t) = \mathrm{Tr}\left\{|f\rangle\langle f|\,\rho_\mathrm{I}(t)\right\} \tag{S1}$$

where $\rho_\mathrm{I}(t)$ is the density matrix in the interaction picture, and where we have taken into account that $|f\rangle\langle f|$ is time-independent in the interaction picture. The Liouville von-Neumann equation for the joint matter + photon reads

$$i\frac{\mathrm{d}}{\mathrm{d}t}\rho_\mathrm{I}(t) = [H_{\mathrm{RM,\,I}}(t), \rho_\mathrm{I}(t)]. \tag{S2}$$

The formal solution to Eq. (S2) is given by

$$\rho_\mathrm{I}(t) = \mathcal{T}e^{-i\int_{t_0}^{t}\mathcal{L}_{\mathrm{RM,\,I}}(t')\,\mathrm{d}t'}\rho_0 = \mathcal{T}e^{-i\int_{t_0}^{t}H_{\mathrm{RM,\,I}}(t')\,\mathrm{d}t'}\rho_0\bar{\mathcal{T}}e^{i\int_{t_0}^{t}H_{\mathrm{RM,\,I}}(t')\,\mathrm{d}t'}. \tag{S3}$$

where $O_{\rm I}(t) = e^{+iH_0(t-t_0)} O e^{-iH_0(t-t_0)}$ and $\mathcal{T}$ ($\bar{\mathcal{T}}$) is the time-ordering (reverse time-ordering) operator. Here $\mathcal{L}_{\rm RM,\,I}(t)\rho = [H_{\rm RM,\,I}(t), \rho]$ is the Liouvillian superoperator.

Using Eq. (S3) in Eq. (S1) leads to

$$P_f(t) = \mathrm{Tr}\left\{ \bar{\mathcal{T}} e^{i\int_{t_0}^{t} H_{\rm RM}(s)\,\mathrm{d}s} \left|f\right\rangle\left\langle f\right| \mathcal{T} e^{-i\int_{t_0}^{t} H_{\rm RM}(s)\,\mathrm{d}s} \rho_0 \right\}, \tag{S4}$$

where we have used the cyclic invariance of the trace $\mathrm{Tr}\{AB\} = \mathrm{Tr}\{BA\}$. To simplify the notation, we have suppressed the subscript I for interaction picture operators, i.e., $O(t) \equiv O_{\rm I}(t)$. Initially, the system is uncorrelated with the external field, $\rho_0 = \left|g\right\rangle\left\langle g\right| \otimes \rho_{\rm R}(0)$. Expanding the exponentials in Eq. (S4) to second-order in the radiation-matter coupling and retaining the terms leading to two-photon absorption yields

$$P_f(t) = \sum_{\mathbf{p}} \int_{t_0}^{t} dt_2 \int_{t_0}^{t_2} dt_1 \int_{t_0}^{t} dt_2' \int_{t_0}^{t_2'} dt_1' \left\langle g|V_{p_4}(t_1')V_{p_3}(t_2')|f\right\rangle \left\langle f|V_{p_2}^{\dagger}(t_2)V_{p_1}^{\dagger}(t_1)|g\right\rangle G_{\mathbf{p}}^{(2)}(t_1', t_2', t_2, t_1) \tag{S5}$$

where $G_{\mathbf{p}}^{(2)}(t_1', t_2', t_2, t_1) = \left\langle \hat{E}_{p_4}^{\dagger}(t_1')\hat{E}_{p_3}^{\dagger}(t_2')\hat{E}_{p_2}(t_2)\hat{E}_{p_1}(t_1) \right\rangle$ is a field correlation function. Equation (S5) can be represented by the time-loop diagram depicted in Fig. 1c. The subscript $\mathbf{p} = p_4p_3p_2p_1$ denotes the sequence of photons (ω_1/ω_2) that interact with the system along the time-loop clockwise. There are four pathways corresponding to $\mathbf{p} = \{\,1221, 1212, 2121, 2112\,\}$, see Fig. 1c. Since $P_f(t) = 0$ for f-states outside the double-excitation manifold, we can sum over all polariton states, which leads to the final compact expression for the ETPA signal

$$S_{\rm ETPA} = \sum_{\mathbf{p}} \int_{t_0}^{t} dt_2 \int_{t_0}^{t_2} dt_1 \int_{t_0}^{t} dt_2' \int_{t_0}^{t_2'} dt_1' C_{\mathbf{p}}(t_1', t_2', t_2, t_1) G_{\mathbf{p}}^{(2)}(t_1', t_2', t_2, t_1) \tag{S6}$$

where $C_{\mathbf{p}}(t_1', t_2', t_2, t_1) = \left\langle V_{p_4}(t_1')V_{p_3}(t_2')V_{p_2}^{\dagger}(t_2)V_{p_1}^{\dagger}(t_1) \right\rangle$ is the four-point dipole correlation function, and where we have used $I = \sum_f \left|f\right\rangle\left\langle f\right|$.

S2. EQ. 5 - SUM-OVER-STATES EXPRESSION FOR THE TRANSITION AMPLITUDE

For initially pure two-photon state $\rho_{\rm R}(0) = \left|\Phi\right\rangle\left\langle\Phi\right|$, the ETPA signal can be recast as the modulus square of a transition amplitude $S_{\rm ETPA} = \sum_f \left|T_{fg}\right|^2$. The transition amplitude for the entangled two-photon absorption reads

$$T_{fg} = \sum_{p_1,p_2} \int_{t_0}^{t} \mathrm{d}t_2 \int_{t_0}^{t_2} \mathrm{d}t_1 \left\langle f|V_{p_2}^{\dagger}(t_2)V_{p_1}^{\dagger}(t_1)|g\right\rangle \left\langle 0|\hat{E}_{p_2}(t_2)\hat{E}_{p_1}(t_1)|\Phi\right\rangle \tag{S7}$$

Using the many-body eigenstates of the polariton Hamiltonian $\{\ |\,i\rangle, i = 0, 1, \cdots\}$ sorted in ascending order of energy $\{\,\omega_i\,\}$, the raising dipole operator $V_n^{\dagger}$ can be written as [1]

$$V_n^{\dagger}(t) = -\sum_{i<j} e^{i\omega_{ji}t} \boldsymbol{\mu}_{ji} \cdot \mathbf{e}_n \left|j\right\rangle\left\langle i\right|. \tag{S8}$$

where $\boldsymbol{\mu}_{ji} = \langle j|\boldsymbol{\mu}|i\rangle$ is the dipole matrix element. Inserting Eq. (S8) into Eq. (S7) yields Eq. (5) in the main text

$$T_{fg}(t) = \sum_{p_1 \neq p_2} \sum_{e} D^{(e)}_{p_2 p_1} \int_{t_0}^{t} \mathrm{d}t_2 e^{i\omega_{fe} t_2} \int_{t_0}^{t_2} \mathrm{d}t_1 e^{i\omega_{eg} t_1} \Phi_{p_2 p_1}(t_2, t_1) \tag{S9}$$

where $\Phi_{p_2 p_1}(t_2, t_1) = \langle 0|\hat{E}_{p_2}(t_2)\hat{E}_{p_1}(t_1)|\Phi\rangle$ is proportional to the amplitude of detecting photon p_1 at t_1 and photon p_2 at t_2. Intuitively, the matter can be taken as a photon detector with a complex inner structure.

It is useful to have the frequency-domain expression for the transition amplitude. The two-photon amplitude in the time domain can be written as

$$\Phi_{p_2 p_1}(t_2, t_1) = \iint \mathrm{d}\omega_2 \mathrm{d}\omega_1 e^{-i\omega_{p_1} t_1} e^{-i\omega_{p_2} t_2} \Phi_{p_2 p_1}(\omega_{p_2}, \omega_{p_1}) \tag{S10}$$

where $\Phi_{p_2 p_1}(\omega_2, \omega_1) \equiv \langle 0|\hat{E}_{p_2}(\omega_2)\hat{E}_{p_1}(\omega_1)|\Phi\rangle$, $\hat{E}_j(t) = \int \mathrm{d}\omega \hat{E}_j(\omega) e^{-i\omega t}$, and $\hat{E}_j(\omega) = i\sqrt{\frac{\omega}{2\epsilon_0 \mathcal{V}}} b_j(\omega)$. Inserting Eq. (S10) into Eq. (S9) leads to the frequency-domain expression for the transition amplitude (up to a global phase)

$$T_{fg} = \sum_{e} \iint \mathrm{d}\omega_1 \, \mathrm{d}\omega_2 \frac{1}{\omega_{fg} - i\gamma_f - \omega_1 - \omega_2} \left(D^{(e)}_{12} \frac{\left\langle 0 \middle| \hat{E}_1(\omega_1)\hat{E}_2(\omega_2) \middle| \Phi \right\rangle}{\omega_{eg} - \omega_2 - i\gamma_e} + D^{(e)}_{21} \frac{\left\langle 0 \middle| \hat{E}_2(\omega_2)\hat{E}_1(\omega_1) \middle| \Phi \right\rangle}{\omega_{eg} - \omega_1 - i\gamma_e} \right) \tag{S11}$$

S3. THE TWIN-PHOTON WAVEFUNCTION

We consider the following twin-photon wavefunction produced by parametric down conversion (PDC) [2, 3]

$$\phi(\omega_1, \omega_2) = \mathcal{N} A(\omega_1 + \omega_2) \mathrm{sinc}\left(\Delta k L/2\right) \tag{S12}$$

where L is the crystal length, $\Delta k = k_{\mathrm{p}} - (k_1 + k_2)$, $A(\omega_1 + \omega_2) = \left(\frac{1}{\sigma\sqrt{\pi}}\right)^{1/2} \exp\left(-\frac{(\omega_1 + \omega_2 - \omega_{\mathrm{p}})^2}{\sigma^2}\right)$ is the normalized pump pulse envelope with bandwidth σ, $\mathrm{sinc}(x) = \sin(x)/x$, $\mathcal{N}$ the normalization constant. For a narrow-band pump $\sigma \to 0$, the spectral envelope

$$A(\omega_1 + \omega_2) \approx \delta(\omega_1 + \omega_2 - \omega_{\mathrm{p}}) \tag{S13}$$

which reflects energy conservation in the PDC process. In type-II down-conversion where $\mathbf{e}_1$ and $\mathbf{e}_2$ are orthogonal, we can expand the wave vector in a Taylor series around the central frequency

$$k_j(\Delta\omega_j + \omega_j^0) \approx k_j(\omega_j^0) + v_j^{-1} \Delta\omega_j, \tag{S14}$$

and the phase-matching condition may be approximated to linear order as

$$\Delta kL/2 = \frac{1}{2}\left(\Delta\omega_1 T_1 + \Delta\omega_2 T_2\right) \tag{S15}$$

where $\Delta\omega_j = \omega_j - \omega_j^0$, and the transit time difference $T_j = L/v_\mathrm{p} - L/v_j$ for $j = 1, 2$ with $v_j = \nabla_{k_j}\omega_j(k_j^0)$ is the group velocity. With Eqs. (S15) and (S13), The PDC two-photon wavefunction generated from a monochromatic pump becomes Eq. (7)

$$\phi(\omega_1, \omega_2) = \mathcal{N}\delta(\omega_1 + \omega_2 - \omega_\mathrm{p})\mathrm{sinc}\left(\frac{\Delta\omega_1 T}{2}\right) \tag{S16}$$

where $T = T_1 - T_2$ is the entanglement time characterising the arrival time delay between the two photons.

In the time domain, the two-photon wavefunction reads

$$\phi(t_1, t_2) \equiv \int \mathrm{d}\omega_1 \int \mathrm{d}\omega_2 e^{-i\omega_1 t_1 - i\omega_2 t_2}\phi(\omega_1, \omega_2) = \frac{2\pi\mathcal{N}}{T} e^{-i\omega_1^0 t_1 - i\omega_2^0 t_2}\Pi\left(\frac{t_1 - t_2}{T}\right) \tag{S17}$$

where the rectangular function $\Pi(x) = 1$ for $-\frac{1}{2} < x < \frac{1}{2}$ and 0 otherwise and ω_i^0 is the central frequency of the i-th beam. Equation (S17) reflects the time-correlation between the entangled photons: the arrival time of each photon is random, but they must arrive together within the entanglement time. Note that the two photons are not time-ordered (ω_1 can come before or after ω_2) as in the quantum light generated by atomic cascade [4].

S3.A. The correlation amplitude

Here we establish the connection between the two-photon correlation amplitude Φ and the two-photon wavefunction ϕ. The two-photon correlation amplitude can be obtained by

$$\begin{aligned}\Phi_{21}(\omega_2, \omega_1) &= \iint \mathrm{d}\omega_1' \,\mathrm{d}\omega_2' \phi(\omega_1', \omega_2') \langle 0|\hat{E}_2(\omega_2)\hat{E}_1(\omega_1) a_1^\dagger(\omega_1') a_2^\dagger(\omega_2')|0\rangle \\ &= -\frac{\sqrt{\omega_2\omega_1}}{2\epsilon_0\mathcal{V}} \iint \mathrm{d}\omega_1' \,\mathrm{d}\omega_2' \phi(\omega_1', \omega_2') \langle 0|a_2(\omega_2) a_1(\omega_1) a_1^\dagger(\omega_1') a_2^\dagger(\omega_2')|0\rangle\end{aligned} \tag{S18}$$

For distinguishable photons,

$$\langle 0|a_2(\omega_2) a_1(\omega_1) a_1^\dagger(\omega_1') a_2^\dagger(\omega_2')|0\rangle = \delta(\omega_1 - \omega_1')\delta(\omega_2 - \omega_2'). \tag{S19}$$

Then

$$\Phi_{21}(\omega_2, \omega_1) = -\frac{\sqrt{\omega_2\omega_1}}{2\epsilon_0\mathcal{V}}\phi(\omega_1, \omega_2) \tag{S20}$$

and in the time-domain

$$\Phi_{21}(t_2, t_1) \approx -\frac{\sqrt{\omega_2^0\omega_1^0}}{2\epsilon_0\mathcal{V}}\phi(t_1, t_2) \tag{S21}$$

where we have invoked the slowly varying approximation

$$\frac{\sqrt{\omega_2\omega_1}}{2\epsilon_0\mathcal{V}} \approx \frac{\sqrt{\omega_2^0\omega_1^0}}{2\epsilon_0\mathcal{V}}. \tag{S22}$$

Similarly,

$$\Phi_{12}(\omega_2,\omega_1) = -\frac{\sqrt{\omega_2\omega_1}}{2\epsilon_0\mathcal{V}}\phi(\omega_2,\omega_1), \tag{S23}$$

and

$$\Phi_{12}(t_2,t_1) = \iint \mathrm{d}\omega_2\mathrm{d}\omega_1 e^{-i\omega_2 t_1}e^{-i\omega_1 t_2}\Phi_{12}(\omega_1,\omega_2) \approx -\frac{\sqrt{\omega_2^0\omega_1^0}}{2\epsilon_0\mathcal{V}}\phi(t_2,t_1) \tag{S24}$$

These relations allow us to obtain the correlation amplitude from the two-photon wavefunction.

1. Indistinguishable photons

The distinguishing characteristics by polarization or arrival time in the entangled photons can be eliminated such that they become indistinguishable [5].

For indistinguishable photons, we can suppress the photon index such that

$$\langle 0|a(\omega_2)a(\omega_1)a^\dagger(\omega_1')a^\dagger(\omega_2')|0\rangle = \delta(\omega_1-\omega_1')\delta(\omega_2-\omega_2') + \delta(\omega_1-\omega_2')\delta(\omega_2-\omega_1'). \tag{S25}$$

Then

$$\Phi_{21}(\omega_2,\omega_1) = \Phi_{12}(\omega_2,\omega_1) = -\frac{\sqrt{\omega_2\omega_1}}{2\epsilon_0\mathcal{V}}\left(\phi(\omega_1,\omega_2)+\phi(\omega_2,\omega_1)\right). \tag{S26}$$

It follows that $\Phi_{12}(t_2,t_1) = \Phi_{21}(t_2,t_1)$ meaning that the transition amplitudes associated with pathways involving the same intermediate state but a different photon sequences coincide. This implies that matter cannot distinguish the interacting photons.

S3.B. Uncorrelated photons

For uncorrelated single photons, the two-photon wavefunction can be factorized as

$$\phi(\omega_1,\omega_2) = \phi_1(\omega_1)\phi_2(\omega_2), \tag{S27}$$

and so is the detection amplitude $\tilde{\Phi}_{p_2p_1}(t,t') \equiv \langle 0|a_{p_2}(t)a_{p_1}(t')|\Phi\rangle$ representing the probability ampliutude of observing photon p_1 at time t' and photon p_2 at time t,

$$\tilde{\Phi}_{p_2p_1}(t,t') \equiv \langle 0|a_{p_2}(t)|\phi_{p_2}\rangle\,\langle 0|a_{p_1}(t')|\phi_{p_1}\rangle\,. \tag{S28}$$

The detection amplitude is proportional to the correlation amplitude under the approximation in Eq. (S22). The single-photon state reads

$$|\phi_j\rangle = \int \mathrm{d}\omega_j \phi_j(\omega_j) b_j^\dagger(\omega_j) \, |0\rangle \tag{S29}$$

where the vaccum corresponds to the modes associated with j-th photon. Inserting Eq. (S29) into Eq. (S28) leads to

$$\begin{aligned}\tilde{\Phi}_{12}(t_1, t_2) &= \langle 0|b_1(t_1)|\varphi\rangle \, \langle 0|b_2(t_2)|\chi\rangle \\ &= \int \mathrm{d}\omega \int \mathrm{d}\omega_1 e^{-i\omega t_1} \varphi(\omega_1) \, \langle 0|b_1(\omega) a_1^\dagger(\omega_1)|0\rangle \int \mathrm{d}\omega' \int \mathrm{d}\omega_2 \chi(\omega_2) e^{-i\omega' t_2} \, \langle 0|b_2(\omega') a_2^\dagger(\omega_2)|0\rangle \\ &= \phi_1(t_1)\phi_2(t_2)\end{aligned} \tag{S30}$$

where $\phi(t) = \int \mathrm{d}\omega e^{-i\omega t}\phi(\omega)$. Similarly,

$$\tilde{\Phi}_{21}(t_1, t_2) = \phi_1(t_2)\phi_2(t_1) \tag{S31}$$

Insering Eqs. (S30) and (S31) into Eq. (S9) leads to the transition amplitude for uncorrelated photons

$$T_{fg} = \frac{\sqrt{\omega_1^0 \omega_2^0}}{2\mathcal{V}\epsilon_0} \sum_e \iint \mathrm{d}\omega_1 \, \mathrm{d}\omega_2 \frac{\phi_1(\omega_1)\phi_2(\omega_2)}{\omega_1 + \omega_2 - \omega_{fg} + i\gamma_f} \left(\frac{D_{12}^{(e)}}{\omega_{eg} - \omega_2 - i\gamma_e} + \frac{D_{21}^{(e)}}{\omega_{eg} - \omega_1 - i\gamma_e} \right) \tag{S32}$$

If the two photons are narrowband with central frequencies ω_j^0 such that

$$\phi(\omega_1) \approx \phi(\omega_1^0)\delta(\omega_1 - \omega_1^0) \tag{S33}$$

the transition amplitude reduces to

$$T_{fg} = \frac{\sqrt{\omega_1^0 \omega_2^0}}{2\mathcal{V}\epsilon_0} \frac{1}{\omega_1^0 + \omega_2^0 - \omega_{fg} + i\gamma_f} \phi_1(\omega_1^0)\phi_2(\omega_2^0) \sum_e \left(D_{12}^{(e)} \frac{1}{\Delta_e^{(2)} - i\gamma_e} + D_{21}^{(e)} \frac{1}{\Delta_e^{(1)} - i\gamma_e} \right) \tag{S34}$$

S3.C. Coherent states

If the photons are in coherent states corresponding to the semiclassical light, the detection amplitude is given by

$$\phi_{p_2 p_1}(t, t') = \langle \phi_{p_2}|a_{p_2}(t)|\phi_{p_2}\rangle \, \langle \phi_{p_1}|a_{p_1}(t')|\phi_{p_1}\rangle \tag{S35}$$

The difference between the coherent state and the single-photon state is that annihilation of an photon does not change the photon state in the former whereas it projects the photon state to the vacuum for the latter.

Coherent states can be generally defined as

$$|\phi_j\rangle = e^{\alpha A_j^\dagger - \alpha_j^* A_j}\,|0\rangle \tag{S36}$$

where $A_j^\dagger \equiv \int_0^\infty \mathrm{d}\omega \mathcal{A}(\omega) b_j^\dagger(\omega)$ is a single-photon creation operator. For a single photon mode,

$$A_j(t) = b_j(\omega). \tag{S37}$$

This corresponds to a monochromatic light. For a continuum of modes,

$$A_j^\dagger = \int \mathrm{d}\omega \phi_j(\omega) b_j^\dagger(\omega) \tag{S38}$$

where $\phi_j(\omega)$ is the normalized spectral envelope. It follows that Eq. (S35) becomes

$$\phi_{21}(t,t') = \int \mathrm{d}\omega_2 e^{-i\omega_2 t}\alpha_2\phi_2(\omega_2) \int \mathrm{d}\omega_1 e^{-i\omega_1 t'}\alpha_1\phi_1(\omega_1) \tag{S39}$$

Realizing that the expectation value of the electric field operator is given by

$$E_j(\omega) = i\sqrt{\frac{\hbar\omega}{2\epsilon_0 \mathcal{V}}}\alpha_j\phi_j(\omega), \tag{S40}$$

Eq. (S39) becomes

$$\Phi_{21}(t,t') = \int \mathrm{d}\omega_2 e^{-i\omega_2 t} E_2(\omega_2) \int \mathrm{d}\omega_1 e^{-i\omega_1 t'} E_1(\omega_1) = E_2(t)E_1(t'). \tag{S41}$$

Equation (S41) implies that the detection amplitude is simply the product of the electric fields, consistent with a semiclassical picture of photon detection theory [6].

The two-photon transition amplitude can be then obtained by inserting Eq. (S41) into Eq. (S34)

$$T_{fg}(t) = \sum_{p_1\neq p_2}\sum_e D^{(e)}_{p_2p_1} \int_{t_0}^{t} \mathrm{d}t_2 e^{i\omega_{fe}t_2} E_{p_2}(t_2) \int_{t_0}^{t_2} \mathrm{d}t_1 e^{i\omega_{eg}t_1} E_{p_1}(t_1) \tag{S42}$$

The corresponding frequency-domain expression reads

$$T_{fg} = \sum_e \iint \mathrm{d}\omega_1\,\mathrm{d}\omega_2 \frac{E_1(\omega_1)E_2(\omega_2)}{\omega_{fg} - i\gamma_f - \omega_1 - \omega_2}\left(\frac{D^{(e)}_{12}}{\omega_{eg} - \omega_2 - i\gamma_e} + \frac{D^{(e)}_{21}}{\omega_{eg} - \omega_1 - i\gamma_e}\right). \tag{S43}$$

Thus, we have obtained the classical two-photon absorption amplitude from a fully quantum mechanical treatment. For monochromatic fields $E_j(\omega_j) = E_j\delta(\omega_j - \omega_j^0)$, Eq. (S43) reduces to

$$T_{fg} = \sum_e \frac{E_1(\omega_1^0)E_2(\omega_2^0)}{\omega_{fg} - i\gamma_f - \omega_1^0 - \omega_2^0}\left(\frac{D^{(e)}_{12}}{\Delta_e^{(2)} - i\gamma_e} + \frac{D^{(e)}_{21}}{\Delta_e^{(1)} - i\gamma_e}\right). \tag{S44}$$

TABLE S1. Expressions for two-photon-absorption signal with quantum and classical light. The photon indexes $p_2p_1 = \{\,21, 12\,\}$ depending on which photon interacts with the matter first.

Time domain	
classical light	$T_{fg}(t) = \sum_{p_1\neq p_2}\sum_e D^{(e)}_{p_2p_1}\int_{t_0}^{t}\mathrm{d}t_2 e^{i\omega_{fe}t_2}E_{p_2}(t_2)\int_{t_0}^{t_2}\mathrm{d}t_1 e^{i\omega_{eg}t_1}E_{p_1}(t_1)$
quantum light	$T_{fg}(t) = \sum_{p_1\neq p_2}\sum_e D^{(e)}_{p_2p_1}\int_{t_0}^{t}\mathrm{d}t_2 e^{i\omega_{fe}t_2}\int_{t_0}^{t_2}\mathrm{d}t_1 e^{i\omega_{eg}t_1}\Phi_{p_2p_1}(t_2,t_1)$
Frequency domain	
classical light	$T_{fg} = -\sum_{p_1\neq p_2}\sum_e \iint \mathrm{d}\omega_1\,\mathrm{d}\omega_2 \frac{E_1(\omega_1)E_2(\omega_2)}{\omega_{fg}-i\gamma_f-\omega_1-\omega_2}\left(\frac{D^{(e)}_{p_2p_1}}{\omega_{eg}-\omega_{p_1}-i\gamma_e}\right)$
quantum light	$T_{fg} = -\sum_e\sum_{p_2\neq p_1}\iint \mathrm{d}\omega_1\,\mathrm{d}\omega_2 \frac{1}{\omega_{fg}-i\gamma_f-\omega_1-\omega_2}\left(D^{(e)}_{p_2p_1}\frac{\langle 0\,\vert\, E_{p_2}(\omega_{p_2})E_{p_1}(\omega_{p_1})\,\vert\,\Phi\rangle}{\omega_{eg}-\omega_{p_1}-i\gamma_e}\right)$

1. Classical light with the same spectral function with quantum light

If the classical light have the same spectral function as in the quantum light,

$$E_j(\omega_j) = E_j^0\frac{T}{2\pi}\mathrm{sinc}\left(\Delta\omega_j T/2\right). \tag{S45}$$

Using the identity $\int_{-\infty}^{+\infty}\mathrm{sinc}\left(\omega T/2\right)e^{-i\omega t}\,\mathrm{d}\omega = \frac{2\pi}{T}\Pi\left(\frac{t}{T}\right)$, the pulse envelope reads

$$E_j(t) = E_j^0 e^{-i\omega_j^0 t}\Pi\left(\frac{t}{T}\right) \tag{S46}$$

Inserting Eq. (S46) into Eq. (S42) leads to the two-photon transition amplitude with two rectangular pulses ($t_0\to-\infty, t\to\infty$)

$$\begin{aligned}
T_{fg} &= E_2^0E_1^0\sum_{p_1\neq p_2}\sum_e D^{(e)}_{p_2p_1}\int_{-\infty}^{\infty}\mathrm{d}t_2 e^{i(\omega_{fe}-\omega^0_{p_2})t_2}\Pi\left(\frac{t_2}{T}\right)\int_{-\infty}^{t_2}\mathrm{d}t_1 e^{i\left(\omega_{eg}-\omega^0_{p_1}\right)t_1}\Pi\left(\frac{t_1}{T}\right)\\
&= E_2^0E_1^0\sum_{p_1\neq p_2}\sum_e D^{(e)}_{p_2p_1}\int_{-T/2}^{T/2}\mathrm{d}t_2 e^{i(\omega_{fe}-\omega^0_{p_2})t_2}\frac{1}{i\Delta_e^{(p_1)}}\left(e^{i\Delta_e^{(p_1)}t_2}-e^{-i\Delta_e^{(p_1)}T/2}\right)\\
&= -E_2^0E_1^0\sum_{p_1\neq p_2}\sum_e D^{(e)}_{p_2p_1}\left(\frac{2i\mathrm{sinc}\left((\omega_{fg}-\omega_1^0-\omega_2^0)T/2\right)}{\omega_{eg}-\omega^0_{p_1}}+\frac{e^{-i(\omega_{eg}-\omega^0_{p_1})T/2}2i\mathrm{sinc}\left((\omega_{fe}-\omega^0_{p_2})T/2\right)}{\omega_{eg}-\omega^0_{p_1}}\right)
\end{aligned} \tag{S47}$$

We have assumed that the pulse duration is shorter than the lifetime, i.e., $T\ll\gamma_e^{-1}$. The first term contains the two-photon resonance condition and thus represents the TPA process whereas the second term contains two single-photon resonances representing a sequential excitation. As shown, for the uncorrelated light, varying the spectral width $1/T$ does not allow modifying the transition amplitude for each transition pathways.

S4. THE BLOCK DIAGONAL POLARITON HAMILTONIAN

S4.A. Two molecules with different transition frequencies

1. Single-polariton block

For $N = 2$ molecules, the subspace Hamiltonian in single-polariton subspace reads

$$H^{(1)} = \begin{bmatrix} \omega_{\rm c} & g_0 & g_0 \\ g_0 & \omega_{\rm a} & 0 \\ g_0 & 0 & \omega_{\rm b} \end{bmatrix} \tag{S48}$$

where g_0 is the single-molecule coupling strength.

2. Two-polariton block

The two-polariton block Hamiltonian spanned by the basis $|gg2\rangle, |eg1\rangle, |ge1\rangle, |ee0\rangle$ reads

$$H^{(2)} = \begin{bmatrix} 2\omega_{\rm c} & \sqrt{2}g_0 & \sqrt{2}g_0 & 0 \\ \sqrt{2}g_0 & \omega_{\rm a}+\omega_{\rm c} & 0 & g_0 \\ \sqrt{2}g_0 & 0 & \omega_{\rm b}+\omega_{\rm c} & g_0 \\ 0 & g_0 & g_0 & \omega_{\rm a}+\omega_{\rm b} \end{bmatrix} \tag{S49}$$

Solving $\det\left(\omega - H^{(2)}\right) = 0$ yields the polariton energies $\omega = 2\omega_{\rm c} \pm \sqrt{\delta^2 + 6g_0^2}, 2\omega_{\rm c}$.

S4.B. Two-polariton block for N identical molecules

We now consider N identical molecules with transition frequency ω_0 and coupling $g_j = g_0$. To understand the structure of the two-polariton states, it is convenient to introduce the collective exciton operators

$$X_j^\dagger = \frac{1}{\sqrt{N}} \sum_{n=1}^{N} e^{ik_j n} \sigma_n^\dagger, \quad j = 0, 1 \cdots, N-1, \tag{S50}$$

where $k_j = 2\pi j/N, j = 0, 1, \cdots, N-1$. The collective exciton operators satisfy the commutation relations

$$[X_i, X_j^\dagger] = -\frac{1}{N} \sum_n e^{i(k_i - k_j)n} \sigma_n^z = \delta_{ij} - \frac{2}{N} \sum_n e^{i(k_i - k_j)n} \sigma_n^\dagger \sigma_n \tag{S51}$$

Since these are different from the boson commutation relations, the excitons cannot in general be considered as bosons. In the low excitation limit of many molecules, i.e., $\sum_{n=1}^{N}\sigma_n^\dagger\sigma_n \ll N$, Eq. (S51) becomes

$$\left[X_i, X_j^\dagger\right] = \delta_{ij} + \mathcal{O}(N^{-1}) \tag{S52}$$

and the collective excitons are approximately bosons.

The upper and lower polaritons are admixtures of the bright exciton state $|\mathrm{X}_0\rangle = X_0^\dagger|G\rangle$, where $|G\rangle$ is the ground state for all molecules, and the cavity mode, with an enhanced splitting $2g_0\sqrt{N}$. The double-excitation manifold contains $\frac{N(N+1)}{2}+1$ states. The polariton Hamiltonian can be recasted in terms of the collective exciton operators

$$H_\mathrm{p} = \omega_0\sum_{j=0}^{N-1}X_j^\dagger X_j + \omega_\mathrm{c}a^\dagger a + g_0\sqrt{N}\left(X_0^\dagger a + X_0 a^\dagger\right). \tag{S53}$$

The double-excitation space can be decomposed into three subspaces spanned, respectively, by

$$\{\ |2\rangle,\ |\mathrm{X}_0 1\rangle,\ |\mathrm{X}_0\mathrm{X}_0\rangle = \sqrt{\frac{N-1}{N}}\left(X_0^\dagger\right)^2\ |g\rangle\ \}, \tag{S54}$$

$\{\ |\mathrm{X}_j\mathrm{X}_0\rangle,\ |\mathrm{X}_j 1\rangle, j\neq 0\ \}$, and $\{\ |\mathrm{X}_j\mathrm{X}_k\rangle, j,k\neq 0\ \}$. The first block comes from excitations of bright excitons and cavity photons and contains three two-polariton states. The subblock Hamiltonian reads

$$H = \begin{bmatrix} 2\omega_c & g_0\sqrt{2N} & 0 \\ g_0\sqrt{2N} & \omega_0+\omega_\mathrm{c} & g_0N/\sqrt{N-1} \\ 0 & g_0N/\sqrt{N-1} & 2\omega_0 \end{bmatrix}. \tag{S55}$$

Eigenvalues of this Hamiltonian Eq. (S55) leads to a pair of upper and lower two-polaritons and one middle two-polariton

$$|f_\mathrm{M}\rangle = \left[\sqrt{\frac{2(N-1)}{3N-2}}, 0, \sqrt{\frac{N}{3N-2}}\right] \tag{S56}$$

at $2\omega_\mathrm{c}$. The enhanced coupling between $|2\rangle$ and $|\mathrm{X}_0 1\rangle$ due to the presence of cavity photons is responsible for the enhanced upper and lower two-polariton splitting.

In addition to this splitting, there is another polariton pair from the second subspace involving dark exciton excitation and cavity photons. The Hamiltonian in this subblock spanned by states $|X_j 1\rangle$ and $|X_j X_0\rangle$ is given by (for each j)

$$H = \begin{bmatrix} \omega_0+\omega_\mathrm{c} & g\sqrt{\frac{N-2}{N}} \\ g\sqrt{\frac{N-2}{N}} & 2\omega_0 \end{bmatrix} \tag{S57}$$

where $g = g_0\sqrt{N}$. The splitting is slightly reduced compared to the vacuum Rabi splitting by a factor of $\sqrt{\frac{N-2}{N}}$. Such states are not dipole connected to the upper and lower polaritons, and cannot be observed in the TPA. The third block involves only dark exciton excitations.

---

[1] Konstantin E. Dorfman, Frank Schlawin, and Shaul Mukamel, "Nonlinear optical signals and spectroscopy with quantum light," Rev. Mod. Phys. **88** (2016).

[2] C. K. Hong and L. Mandel, "Theory of parametric frequency down conversion of light," Phys. Rev. A **31**, 2409–2418 (1985).

[3] Timothy E. Keller and Morton H. Rubin, "Theory of two-photon entanglement for spontaneous parametric down-conversion driven by a narrow pump pulse," Phys. Rev. A **56**, 1534–1541 (1997).

[4] Ashok Muthukrishnan, Girish S. Agarwal, and Marlan O. Scully, "Inducing Disallowed Two-Atom Transitions with Temporally Entangled Photons," Phys. Rev. Lett. **93**, 093002 (2004).

[5] W. P. Grice, A. B. U'Ren, and I. A. Walmsley, "Eliminating frequency and space-time correlations in multiphoton states," Phys. Rev. A **64**, 063815 (2001).

[6] Roy J. Glauber, "The Quantum Theory of Optical Coherence," Phys. Rev. **130**, 2529–2539 (1963).